Journal of Petroleum Science and Engineering, Volume 162, March 2018, pp.1-11
DOI:10.1016/j.petrol.2017.12.019

Scale-up and turbulence modelling in pipes

X.F. Loyseau[a], P.G. Verdin[a,*], L.D. Brown[b]

[a]*School of Water, Energy and Environment, Cranfield University, Bedfordshire, MK43 0AL, UK*
[b]*Science Deployed LLC, Katy, TX 77494, USA*

Abstract

Large diameter pipes are commonly used for oil and gas transportation. Experimental and numerical results, including turbulence properties, are often obtained for small diameter pipes. Only little information is available for pipes larger or equal to 200 mm. Results obtained with Reynolds Averaged Navier-Stokes (RANS) turbulence models for single phase flow in pipes of different sizes are presented and discussed. The use of non-dimensional data is usually assumed sufficient to present general information and is assumed valid for any size of pipe. The validity of such assumptions has been checked and the flow behaviour in small, medium and large pipes obtained with several of the most common RANS turbulence models, has been established under specific conditions via Computational Fluid Dynamics (CFD) techniques. Although difficulties were sometimes encountered to reproduce correctly the turbulence properties described in the literature with the turbulence models implemented in open source CFD codes, it is shown that a scaling-up approach is valid as the general flow pattern can be predicted by a non-dimensional strategy.

Keywords: CFD model, pipe, turbulence, simulation, scale-up, non-dimensional

1. Introduction

Results obtained with different turbulence models and compared with experimental data are legion in the literature for small diameter pipes, see for instance Hrenya *et al.* (1995); Spalart (2000); Pope (2001); Karvinen & Ahlstedt (2008); Vijiapurapu & Cui (2010); Escue & Cui (2010). Some numerical work has been performed for large diameter pipes (Brown *et al.*, 2009; Verdin *et al.*, 2014; Guan *et al.*, 2015), however, published studies of the behaviour of turbulence models in pipes larger or equal to 200 mm, such as from Shawkat *et al.* (2008), are rare.

The flow can be laminar or turbulent. Between these two regimes, there is a transition region, which has been found experimentally to be a function of the Reynolds (Reynolds, 1883) number $Re = \rho UL/\mu$, ρ being the fluid density, U its velocity, μ its dynamic viscosity and L a characteristic length, equal to the hydraulic diameter of the pipe D_h when a pipe flow is considered. For such geometries, the flow is assumed turbulent when the Reynolds number is higher than $4,000$ and a transition from laminar to turbulent is present when $2,300 < Re < 4,000$.

Experiments being restricted to small diameter pipes, numerical approaches are usually used for studies of the flow in medium and large diameter pipes. Although Large Eddy Simulations (LES) and Direct Numerical Simulations (DNS) solve the spatially averaged and the full Navier-Stokes equations respectively, they also require more time and computing resources compared to Reynolds Averaged Navier-Stokes (RANS) based simulations. Their use is therefore often restricted to simple geometries and relatively low Reynolds numbers flows, as pointed out by Ahn *et al.* (2015).

The aim of the work presented here is to palliate the lack of information for medium and large pipes and to provide a set of RANS based results for single phase flow in pipes of different sizes. This will be achieved through the use of Computational Fluid Dynamics (CFD) which is used extensively to study macroscopic hydraulics phenomena in industrial systems. Near the walls (where the non-dimensional distance to the wall is $y^+ = u^* y/\nu < 100$, with u^*

*Corresponding author. Tel: +44 (0)1234 75011 ext.5214
Email address: p.verdin@cranfield.ac.uk (P.G. Verdin)

Nomenclature

D	Pipe diameter, m
D_h	Hydraulic diameter, m
L	Fully developped flow length, m
ΔP	Pressure drop, Pa
k	Turbulent kinetic energy, J/kg
u	Velocity, m/s
u^*	Friction velocity, $(= \sqrt{(\tau_w/\rho)})$
u_{bulk}	Velocity in the bulk flow, m/s
y	Normal distance from the wall, m

Dimensionless numbers

k^+	Turbulent kinetic energy
Re	Reynolds number, $(= \rho u D_h/\mu)$
u^+	Velocity, $(= u/u^*)$
y^+	Wall distance, $(= u^* y/\nu)$

Greek letters

ϵ	Turbulence dissipation rate, $J/kg - s$
μ	Dynamic viscosity, $Pa - s$
ν	Kinematic viscosity, $(= \mu/\rho)$
ω	Specific turbulence dissipation, $1/s$
ρ	Density, kg/m^3
τ_w	Wall shear stress, Pa

Friction factor

f_D	Darcy-Weisbach
f_f	Fanning

the friction velocity, y the normal distance from the wall and $\nu = \mu/\rho$ the kinematic viscosity), the turbulence affects quantities such as pressure gradient, heat transfer and when present, droplets deposition. The friction velocity (also known as the shear-stress velocity) $u^* = \sqrt{\tau_w/\rho}$, is used for the non-dimensional scaling in turbulent flows, τ_w being the shear stress at the wall.

Another objective of this research work is to discuss the validity of a non-dimensional approach established for small diameter pipes when the pipe diameter is increased. More explicitly, the values used for the non-dimensional strategy obtained from the simulations will be discussed as such values are dependent on the mesh structure in the near-wall region.

2. Turbulence models

Most of the earliest research in the field of turbulent wall-bounded flows was purely theoretical, such as the pioneering work of Prandtl in 1904 who introduced the concept of boundary layers and the work from von Karman in the 1930s who formulated the law of the wall. According to the law of the wall, the wall region is divided into a viscous sublayer attaining a linear profile, a logarithmic-law region with a buffer layer in between, and finally an outer layer (El Khoury *et al.*, 2014), see Figure 1. Large variations of the velocity and turbulent characteristic fields occur next to the wall. Based on the region that needs to be resolved, the location of the first cell adjacent to the wall is determined. The near-wall mesh resolution dictates the choice turbulence modeling strategies: Boundary Layer (BL)-type correlation (also called "wall-functions"), or "near-wall" models (also called low-Reynolds number models) for coarse or fine grids respectively. These two approaches are classically incompatible: near-wall models often rely on high-order derivative terms to represent turbulent production and transport, which compromises robustness on a coarse grid (Billard *et al.*, 2015). Wall functions are semi-empirical expressions which bridge the viscosity-affected region between the wall and the fully-turbulent region. The main benefit in using these wall functions lies in the significant reduction in mesh resolution and thus reduction of simulation time.

The low-Reynolds $k - \varepsilon$, $k - \omega$ SST, BL-v^2/k and RSM (Reynolds Stress) RANS turbulence models have been applied here; a short derivation of these models can be found in Salehi *et al.* (2017). The low-Reynolds $k - \varepsilon$, with k the turbulent kinetic energy and ϵ the turbulence dissipation rate, is one of the most common models. The Launder-Sharma (Launder & Sharma, 1974) is a variant known as the standard $k - \varepsilon$ model. This model can be

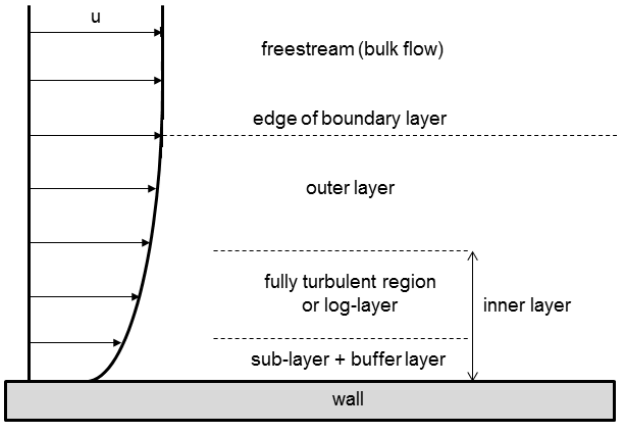

Figure 1: Regions forming the turbulent boundary layer

inaccurate, especially in case of large pressure gradients but is numerically stable and fast, so is widely used for industrial applications.

The Wilcox $k-\omega$ (Wilcox, 1988) is a commonly used two-equation model where one equation solves the transport of the turbulent kinetic energy k and the other one solves the specific dissipation ω. The Shear Stress Transport (SST), variant of the $k-\omega$ model, has been developed by Menter (1994). This model switches automatically from a $k-\omega$ formulation near the walls to the $k-\varepsilon$ definition in the bulk flow. This makes this model directly usable in the viscous sub-layer and can therefore be used as a low-Reynolds turbulence model and thus avoids sensitivity problems encountered by a k-ω formulation due to inlet turbulence properties (ANSYS, 2013).

The $k-\epsilon-v^2/k$ also denoted BL-v^2/k (Billard & Laurence, 2012) is a near-wall eddy viscosity RANS model based on the elliptic blending method. It applies in a near-wall eddy viscosity (EVM) framework the elliptic blending (EB) method proposed by Manceau & Hanjalic (2002) in their Reynolds stress model. It resolves v^2/k, whose quadratic behaviour similar to that of k, is easier to capture.

The Reynolds stress model (RSM) (Launder *et al.*, 1975; Gibson & Launder, 1978) is one of the most elaborate turbulence models. It closes the Reynolds-averaged Navier-Stokes equations by solving transport equations for the Reynolds stresses, together with an equation for the dissipation rate ϵ. This model is particularly useful when the flow features of interest are the result of anisotropy in the Reynolds stresses (ANSYS, 2013). Low Reynolds versions of the Reynolds Stress model exist. However, the high Reynolds formulation is most widely encountered and is usually based on wall functions.

Commercial and open source solvers do not always share the same approaches. The open source CFD code OpenFOAM (Weller & Tabor, 1998) for instance only uses log-wall-functions, which are inappropriate for refined walls (applying a log layer profile in the viscous layer is not correct.). However, the commercial code FLUENT (ANSYS, 2013) proposes linear wall functions alongside log-wall-functions. The wall formulation is modified in FLUENT from the original formulation of Launder-Reece-Rodi (Launder *et al.*, 1975) to make it more robust, while OpenFOAM still uses the original formulation.

When using low Reynolds models or any model with enhanced wall treatment, the average y^+ value should be around 1 (and up to 5) to ensure the laminar sub-layer is well captured. To generate a suitable mesh, the friction velocity u^* has to be determined. Two methods are commonly used to evaluate this quantity which is approximately constant in the near-wall region for turbulent flows. The friction velocity scale-based estimation which is the simplest and fastest one, is based on the near wall gradient, pressure gradient, and for the pre-processing part, on correlations (Blasius (1913) for instance). The second approach is the two friction velocity scale estimation which tries to take into account turbulence effects (Code_Saturne, 2015). The first method is more appropriate for a boundary layer resolved mesh while the latter is best for a wall-function based mesh.

Meshes comprising a first cell height such as $y^+ = 1$ were constructed based on the friction velocity obtained from the Blasius correlation, described in Section 3. Simulated results, however, often showed discrepancies when

compared to the Blasius estimates and the first cell height was usually found slightly below or higher than $y^+ = 1$. Other meshes were generated and used with wall functions, with a first cell center height around $y^+ = 20$, although values should ideally be within the log-law layer, i.e. between 30 and 300.

All data provided in this paper are non-dimensionalised using the friction velocity from the simulations. A formulation has been adopted, which considers two components which are taken into account: the pressure drop as it is often more reliably computed, and the mesh quality as the manual evaluation is dependent on the near wall cell spacing. The "manual" value can be established through calculating the velocity gradient at the wall which can be determined with the velocity values at the center of the first 3 cells in the direction normal to the wall and with the distance to the wall of each cell center considered. Based on the wall shear stress expression (Equation 1 defined in the next section) and using $u^* = \sqrt{\tau_w/\rho}$ defined earlier, the "manual" u^* value can be calculated. When "manual" and "pressure-based" methods are specified, the friction velocity used for the non-dimensionalisation is $u^* = (u^*_{manual} + u^*_{pressure})/2$. Such procedure aims at limiting potential errors when using either the first formulation or the second formulation only. Additional information on difficulties inherent to the evaluation of u^* is provided in the next section.

3. Non-dimensionalisation process

Non-dimensional quantities have been defined to allow a comparison with existing data from the literature, usually written in a non-dimensional form. In the case of bounded flows, expressions derived from the momentum equations allow an analytical study of the near-wall behavior, through the use of non-dimensionalisation. The wall shear stress is expressed as:

$$\tau_w = \mu \left.\frac{\partial u}{\partial y}\right|_w , \tag{1}$$

where the subscript w stands for the wall, u is the flow velocity along the wall, μ is the fluid dynamic viscosity and y the normal distance from the wall.

The Blasius correlation can be used to evaluate the wall shear stress in smooth wall pipes:

$$\tau_w \approx f_f \cdot \rho \frac{u^2_{bulk}}{2} , \tag{2}$$

with u_{bulk} the velocity in the bulk flow and the Fanning friction factor f_f defined as:

$$f_f = \frac{f_D}{4} = \begin{cases} \dfrac{16}{Re} & \text{if } Re < 3,000 \quad (3a) \\ \dfrac{0.3164}{4} \cdot Re^{-1/4} & \text{if } Re > 3,000 \quad (3b) \end{cases}$$

with Re the Reynolds number based on the hydraulic diameter D_h, and f_D the Darcy-Weisbach factor.

As mentioned previously, it is critical to be able to correctly assess the near-wall quantities, and one of the most important ones is the friction velocity u^*. Despite correlations being available for most common cases, each model of turbulence will produce a different result and will therefore generate a different wall velocity gradient. Numerically, when the mesh is sufficiently refined at the wall, the velocity gradient can be retrieved directly. However, for meshes where the turbulence model imposes a first cell around $y^+ = 20$, another method should be used. The easiest approach is to use correlations relating the pressure gradient to the friction velocity. The friction velocities, reported later in this document, are all based on the following correlation resulting from $u^* = \sqrt{\tau_w/\rho}$ and assuming a simple balance between pressure-force and wall-friction-force in steady state, fully developed straight pipe incompressible single phase flow:

$$u^* = \sqrt{\frac{D\Delta P}{4\rho L}} , \tag{4}$$

where D is the pipe diameter, ΔP is the pressure drop over a distance L where the flow is fully developed and ρ is the fluid density.

For cases where the first cell center is such that $y^+ \geq 20$, Code_Saturne evaluates the friction velocity using expressions involving the turbulent kinetic estimate in the first cell (Code_Saturne, 2015). The friction velocity obtained through this method is not reported here as it is assumed that errors in the prediction of the turbulent kinetic energy could significantly impact the results.

As each method described above can generate slightly different results, large differences are sometimes encountered when reporting the non-dimensional data. Although pressure drop and shear stress values can be obtained from the simulation, they depend on numerical aspects such as the first cell spacing at the wall. Discrepancies might appear between the u^* value obtained from Equation 4, the value predicted automatically by the CFD software and the value calculated manually when computing the velocity gradient and applying Equation 1. Such errors can also be encountered with experimental work as highlighted by (Den Toonder & Nieuwstadt, 1997) who stated that the use of experimental velocity data to compute u^* might lead to systematic errors in the turbulence statistics plotted in wall variables. To check and and prevent erroneous estimates of the friction velocity, numerical-based results were compared to those obtained with Blasius correlations. Such comparisons are valid as all simulations were performed in smooth pipes.

4. 0.5 in. ($\simeq$ 12.7mm) diameter pipe

Experimental data are generally obtained in small diameter pipes. Such geometries are investigated first in this work as numerical results can easily be compared to available data from the literature. A five meter long vertical pipe of diameter 0.5 in. has been selected to validate the flow solution (Matida *et al.*, 2000). The Reynolds number is $Re \simeq 12,965$ and the pipe wall is assumed smooth. Different meshes were generated and information relative to their structure are provided. This includes the total number of cells in the domain, the length of the pipe and the first cell center-wall distance. The y^+ value deduced from the Blasius relation is also provided for each mesh considered.

Flow conditions are reported in Table 1. Periodic boundary conditions have been applied at the inlet and outlet sections of the pipe to ensure that the flow is fully developed inside the whole domain. The SIMPLE algorithm was run until convergence, with a 10^{-6} convergence criterion.

Table 1: Flow conditions for air

u (m/s)	ρ (kg/m^3)	μ $(Pa.s)$	Re $(-)$
15.66	1.2	$1.84\ 10^{-5}$	12,965

A mesh-independence study has been performed with the open source CFD solver OpenFOAM and the k-ω SST turbulence model. The flow solution obtained with a mesh comprising 760,500 cells has been found suitable for further analysis, see Figure 2. Both meshes comprising 361,000 cells and 464,000 cells could also have been used here for a "general" study of the flow quantities. However, as the finer one (760,500 cells) is also further refined in the axial direction, this mesh has been preferred to comply with the $y^+ < 1$ condition, the non-dimensional distance to the wall derived from Blasius being $y^+ = 0.8$. This mesh has also been successfully used for droplets transport studies, see Loyseau & Verdin (2016) for details.

Several turbulence models implemented in OpenFOAM and in another open source CFD solver, Code_Saturne, were tested. The Launder-Sharma k-ε (Launder & Sharma, 1974) and the shear stress transport (SST) k-ω (Menter, 1994) models were both able to predict a pressure gradient in agreement with the Blasius correlation for smooth walls (Equation 2), which predicts a wall shear stress around 1.08 Pa, and a pressure gradient of 344 Pa/m. Equation 4 provides an estimated friction velocity for this case, around 0.95 m/s. To check that the flow solution is well calculated with OpenFOAM, the pipe outlet velocity profile obtained with the open source code has been compared to the velocity profile generated with the industry standard flow solver FLUENT, considering the same three-dimensional mesh and turbulence model. As can be seen from Figure 3, velocity profiles are identical with both numerical codes.

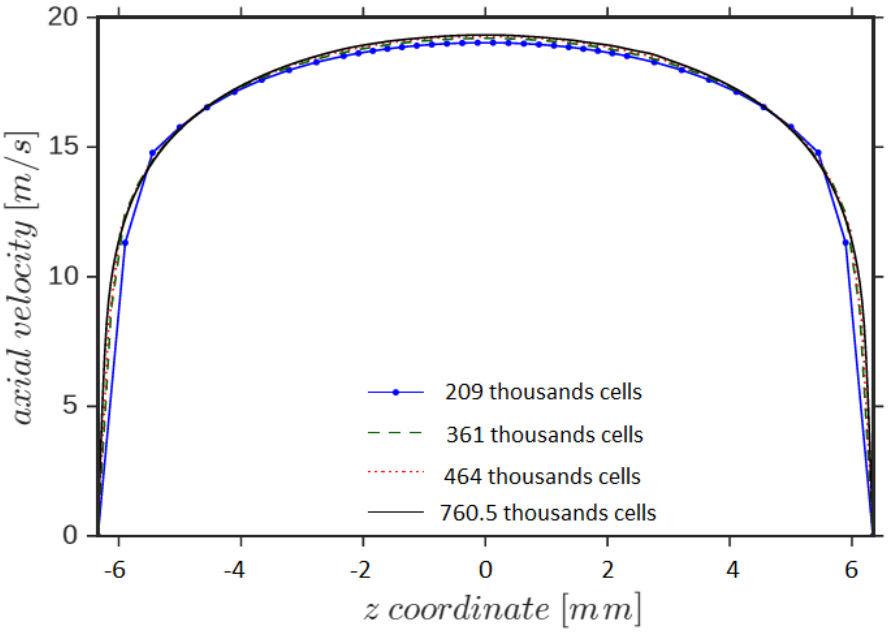

Figure 2: Axial velocities obtained with different meshes plotted along the direction perpendicular to the axial axis

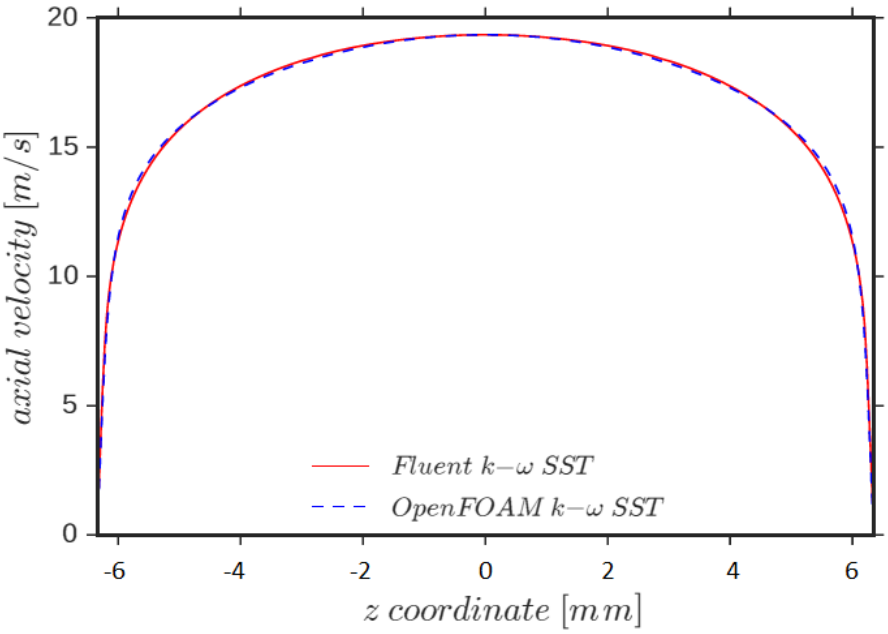

Figure 3: Velocity profiles with OpenFOAM and FLUENT

It appeared important to understand how a particular mesh used with a given turbulence model behaves with various flow solvers. To achieve this objective, simulations were also performed with Code_Saturne. However, because of compatibility issues, meshes generated for a specific flow solver cannot always be used with another flow solver. Two meshes were therefore generated with the mesh generator Salome (2015), which is fully compatible with Code_Saturne, for simulations performed with the $k-\omega$ SST and BL-v^2/k models, and the $k-\varepsilon$ model, respectively. The first mesh, used for the $k-\omega$ SST and the BL-v^2/k models, is the finest one, comprising around 1M cells, with $y^+ = 0.41$. The second one is coarser (around 0.5M cells) and is used for the $k-\varepsilon$ based simulation, with $y^+ = 6.7$.

Figure 4 shows the resulting velocity profile plotted in the radial direction from the center of the pipe (z=0) to the wall (z=R=6.35mm). Although being obtained with different meshes and software, it appears clearly that the velocity profile is nearly identical for simulations run with all three turbulence models.

The velocity gradient at the wall could be determined and used to get the friction velocity and the non-dimensional velocity $u^+ = u/u^*$. Figure 5 shows the simulation-based results which can be compared to theoretical asymptotic values (details available in Benedict (1980) and Zagarola *et al.* (1997)). Results for $y^+ \leq 5$, i.e. for $u^+ = y^+$, are located in the viscous sublayer. For those such as $5 < y^+ < 30$ represented by $u^+ = (1/0.436)ln(y^+)$, they are located in the buffer layer. When $y^+ > 30$, described through the equation $u^+ = 2.5ln(y^+) + 5.5$, results are located in the turbulent dominated layer.

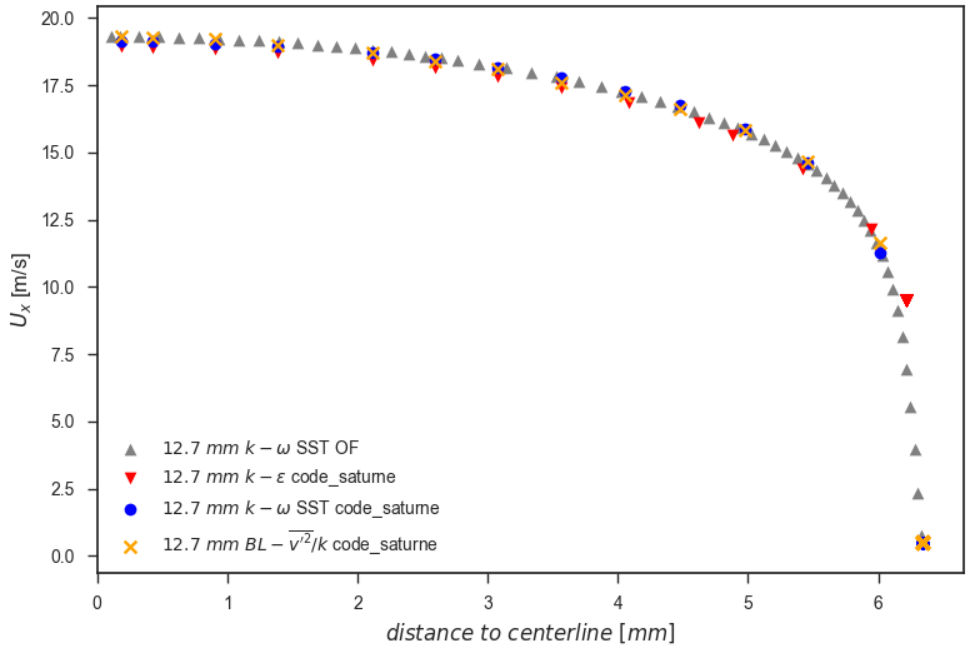

Figure 4: Axial velocity profiles in the 0.5 in. pipe

From all models tested, the $k-\omega$ formulation seems to show the closest match with the theoretical values and to the experimental data reported in Eggels *et al.* (1994). As mentioned previously, a y^+ value under 1 (for a near wall refinement option) or above 30 (when using wall functions) should ideally be obtained. However, a value $y^+ = 6.7$ is achieved with the $k-\varepsilon$ model, which is in the transition region (as shown on Figure 5). Results obtained with this turbulence model are nevertheless acceptable in the core flow, see Figure 4. The BL-v^2/k-based velocity profile also shows a good match with other numerical-based dimensional velocity profiles in the core flow. However, the non-dimensional values of velocity obtained with this model differ with other turbulence-based results in the turbulent dominated layer, see Figure 5. This difference could be inherent to the non-dimensionalisation procedure, where the friction velocity u^*, as explained previously, is difficult to obtain with accuracy.

The turbulent kinetic energy representation allows a comparison of all turbulence models, including those which are not able to predict the perturbation velocity of components u', v' and w'. The turbulence kinetic energy calculated

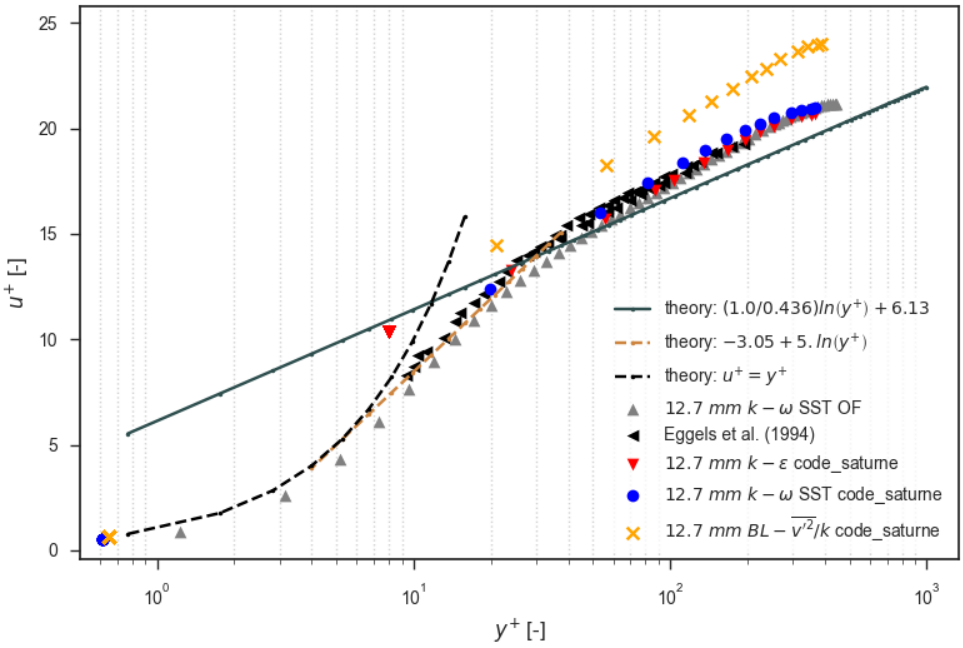

Figure 5: Non-dimensional axial velocity profiles in the 0.5 in. pipe

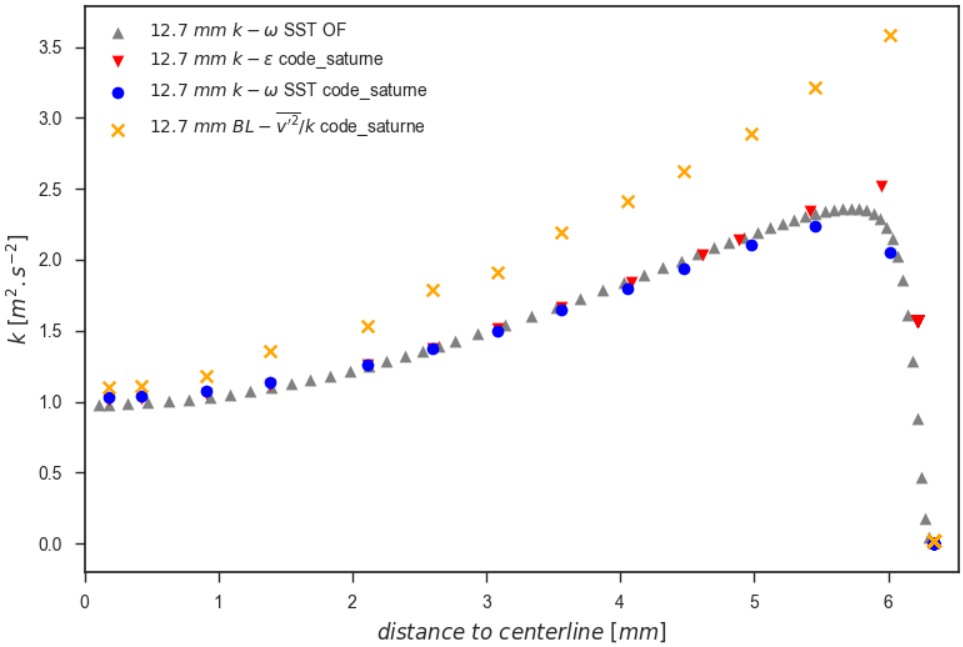

Figure 6: Turbulent kinetic energy in the 0.5 in. pipe

with all models is plotted in Figure 6. As expected, the choice of turbulence model highly affects the prediction of this quantity. Most models tested, apart from BL-v^2/f which predicts higher levels of turbulent kinetic energy near the walls, produce similar dimensional results. Figure 7 shows the corresponding non-dimensional values ($k^+ = k/u^{*2}$) which are compared to a DNS carried out by Kim *et al.* (1987) for a lower Reynolds number: $Re = 6,600$. DNS

results have been used here for comparison purposes as it has proven difficult to identify experimental-based k^+ in the literature. However, Eggels *et al.* (1994) demonstrated that DNS results from different authors, including Kim *et al.* (1987), showed a good agreement with experimental data.

A peak is present in all plots shown in Figure 7. As claimed by Hultmark *et al.* (2010) who performed a set of experiments in fully developed pipe flows, a near-wall peak is present around $y^+ = 16$ and this peak is nearly invariant with Reynolds number in location and magnitude at Reynolds numbers up to 145,000. The Reynolds numbers encountered in the current study are far below this value, showing that the DNS results from Kim *et al.* (1987) concur with conclusions of Hultmark *et al.* (2010) in terms of peak location.

For this size of pipe, it can clearly be established from Figure 7 that no single model tested here was able to correctly and simultaneously predict both the peak radial position (around $y^+ = 16$) and the k^+ peak value (around $k^+ = 4.3$) established by Kim *et al.* (1987). Results obtained with the $k-\varepsilon$ and $k-\omega$ SST models are under-predicted and those from BL-v^2/f are over-predicted when compared to the DNS-based results. All models present a shift of the k^+ peak when compared to Kim *et al.* (1987).

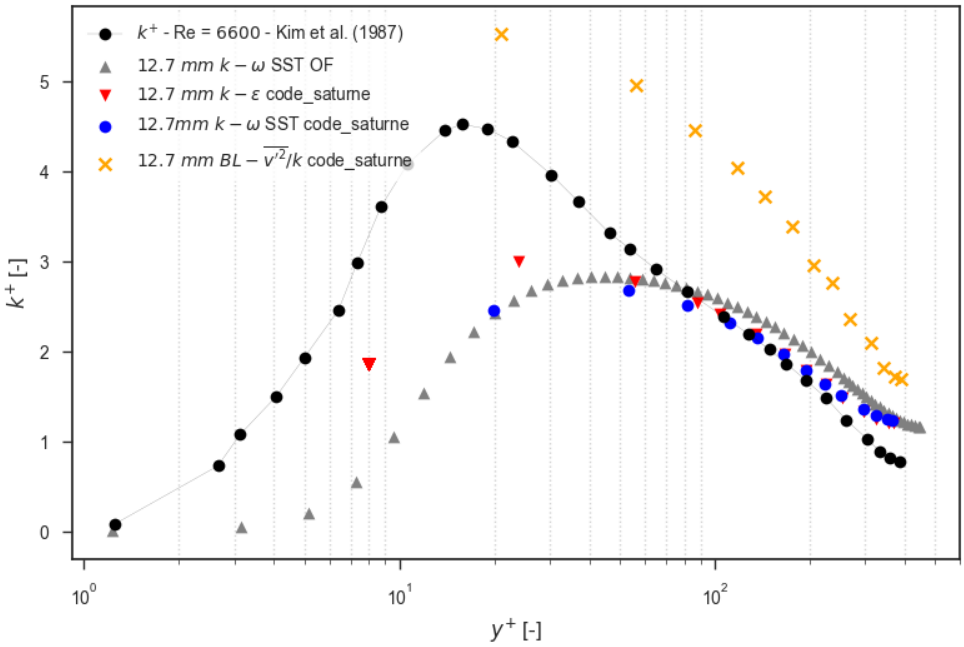

Figure 7: Non-dimensional turbulent kinetic energy in the 0.5 in. pipe

Friction velocity and pressure gradient values could be extracted from all simulations, they are reported in Table 2 along with the values obtained with the Blasius correlation. When looking at the friction velocity, results obtained with all turbulence models are very close. The lowest friction velocity is obtained with BL-v^2/k (Code_Saturne). Similarly, the pressure gradient is the lowest with the BL-v^2/k (Code_Saturne) model while other models predict a value close to the Blasius correlation. At this stage, based on the results presented in this table and on the previous discussion about the non-dimensional axial velocity, the $k-\omega$ SST seems to be the most suitable model for this study.

Table 2: Simulation results for the 0.5 in. pipe

Turbulence model	Predicted friction velocity (m/s)		Predicted pressure gradient (Pa/m)
	manual	pressure-based	
BL-v^2/k (Code_Saturne)	0.8050	0.8536	275.57
$k-\omega$ SST (Code_Saturne)	0.9347	0.9310	327.79
$k-\omega$ SST (OpenFOAM)	0.9484	0.9531	343.55
$k-\varepsilon$ (Code_Saturne)	1.1270	0.9344	330.22
Blasius correlation	0.9500		342.65

5. 14.5 in. (≃ 36.83cm) diameter pipe

A transition between small diameter pipes and large diameter pipes should be established for a better comparison and discussion on a scaling-up strategy from laboratory-type models to large industrial-type models. Medium size diameter pipes are however rarely studied experimentally or numerically. Despite the lack of data available for validation, a vertical pipe of diameter 14.5 in. has been considered. The flow conditions used for this case are written in Table 3. The Blasius correlation (smooth walls) predicts a wall shear stress around 2.25 Pa, leading to a friction velocity of 0.05 m/s and a pressure gradient around 24 Pa/m.

Table 3: Flow conditions for oil in pipe

u (m/s)	ρ (kg/m^3)	μ $(Pa.s)$	Re $(-)$
0.84	868.8	2.0×10^{-2}	13,460

Similarly to the 0.5 in. cases, different meshes have been created for the 14.5 in. diameter pipes, depending on the flow solver and turbulence model selected. For all cases considered, the pipe is 20 m long to ensure that the flow has enough length to develop fully. The first mesh which comprises around 300,000 cells, has a y^+ value of 0.64, and has been used with the BL-v^2/k, $k-\omega$ SST and $k-\varepsilon$ models in Code_Saturne. The second mesh is made of 700,000 cells, with a y^+ value of 6.17 and has been used with the $k-\omega$ SST in OpenFOAM. Finally, the third mesh comprises around 720,000 cells and shows a y^+ value of 2.9. This mesh has been used for simulations performed in FLUENT with the Reynolds stress model.

Figure 8 shows the velocity profiles obtained with several turbulence models, including the Reynolds Stress model (RSM) from FLUENT. As can be noticed, the prediction from the $k-\varepsilon$ model in Code_Saturne is significantly diverging from other predictions, suggesting that this model performs poorly. However, the estimates from $k-\omega$ SST and BL-v^2/k from Code_Saturne, and the $k-\omega$ SST from OpenFOAM, are in agreement with the RSM-based profile from FLUENT; only a slight difference is visible in the central region of the pipe, where the velocity profile is flatter for the FLUENT case.

When comparing the dimensionless velocity with the theoretical asymptotic values and the experimental data reported in Eggels *et al.* (1994) in Figure 9, it appears that the $k-\omega$ SST based results from Code_Saturne and the RSM from FLUENT are fairly close to the theoretical and experimental values. The $k-\omega$ SST model in OpenFOAM also performs fairly well, especially when $y^+ > 60$. Not surprisingly, the RSM from FLUENT performs better than any other RANS model investigated since it is the only model which takes into account the full anisotropic turbulence of the flow.

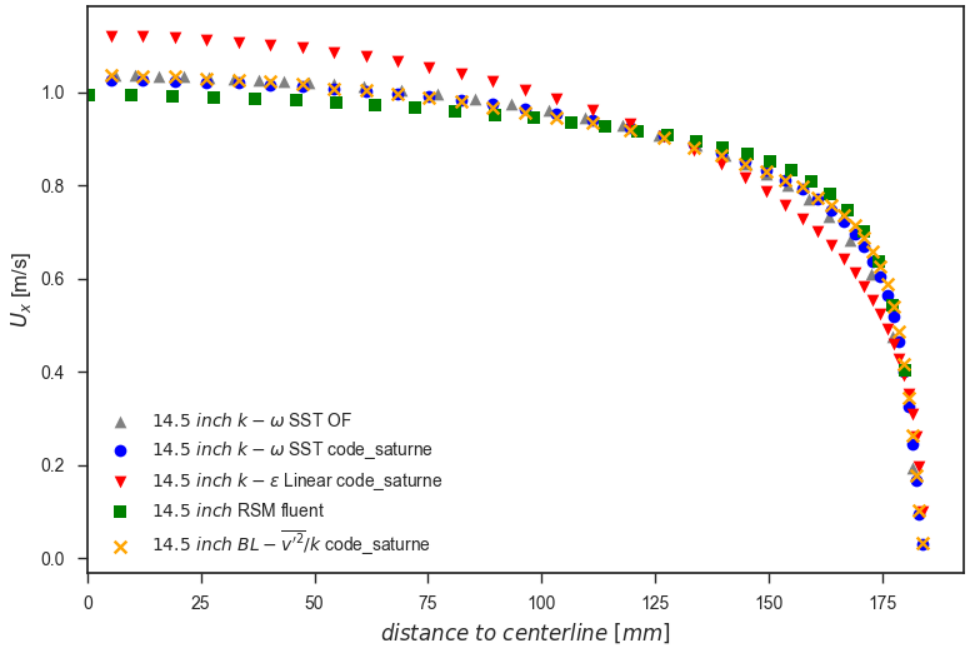

Figure 8: Axial velocity profiles in the 14.5 in. pipe

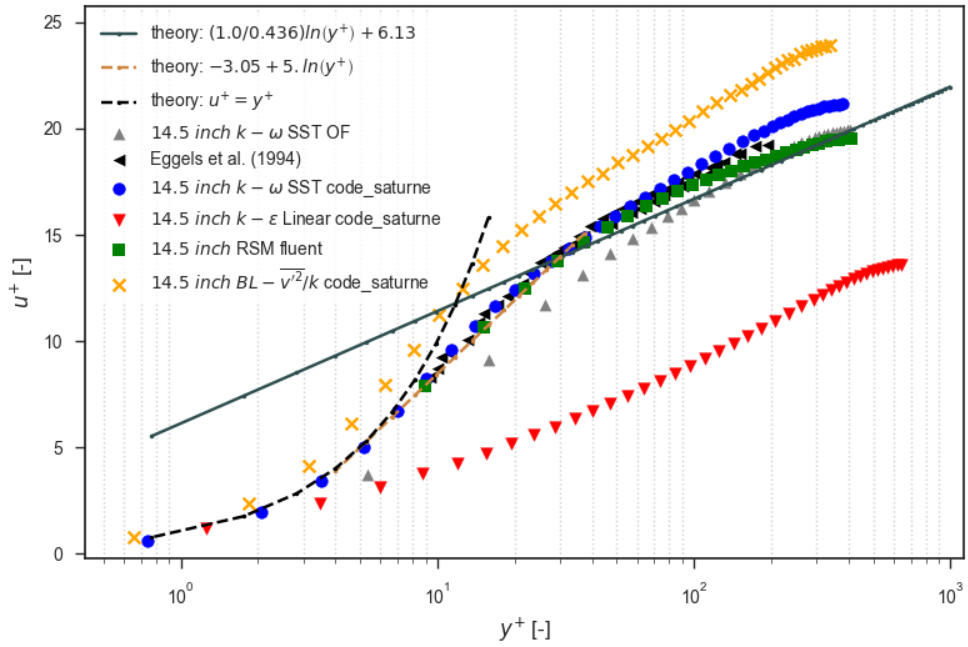

Figure 9: Non-dimensional axial velocity profiles in the 14.5 in. pipe

The BL-v^2/k model results do not compare well with either the theoretical or the experimental values when $y^+ > 10$, i.e. in the buffer and in the turbulent dominated layers. The u^+ profile obtained with this turbulence model is very similar to the one obtained previously for a small diameter pipe. Once again, the discrepancies observed here could be due to the difficulties to determine an accurate friction velocity value used for the non-dimensionalisation

procedure, when using this turbulence model.

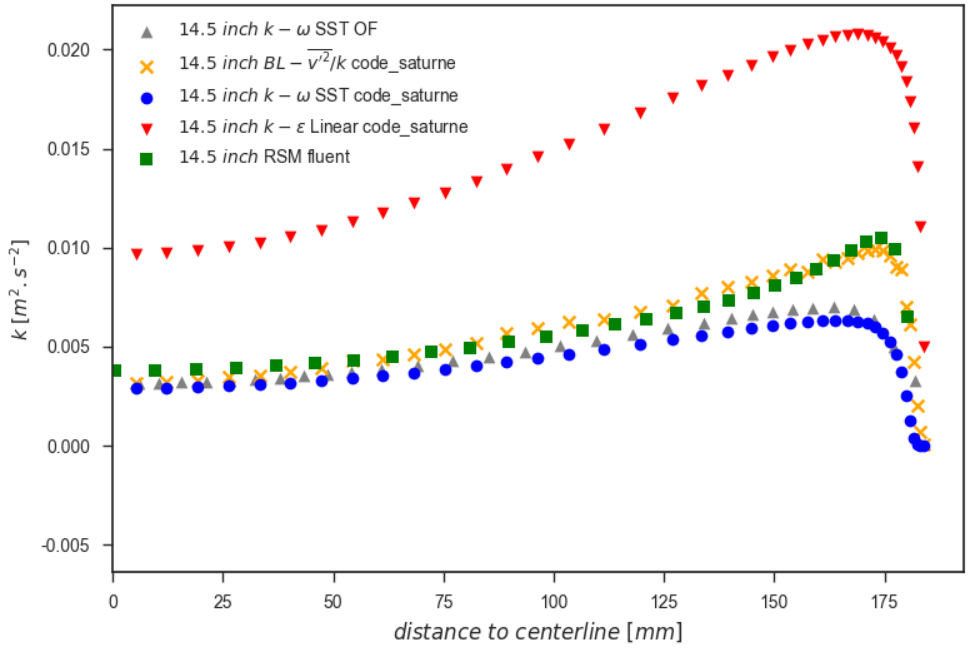

Figure 10: Turbulent kinetic energy in the 14.5 in. pipe

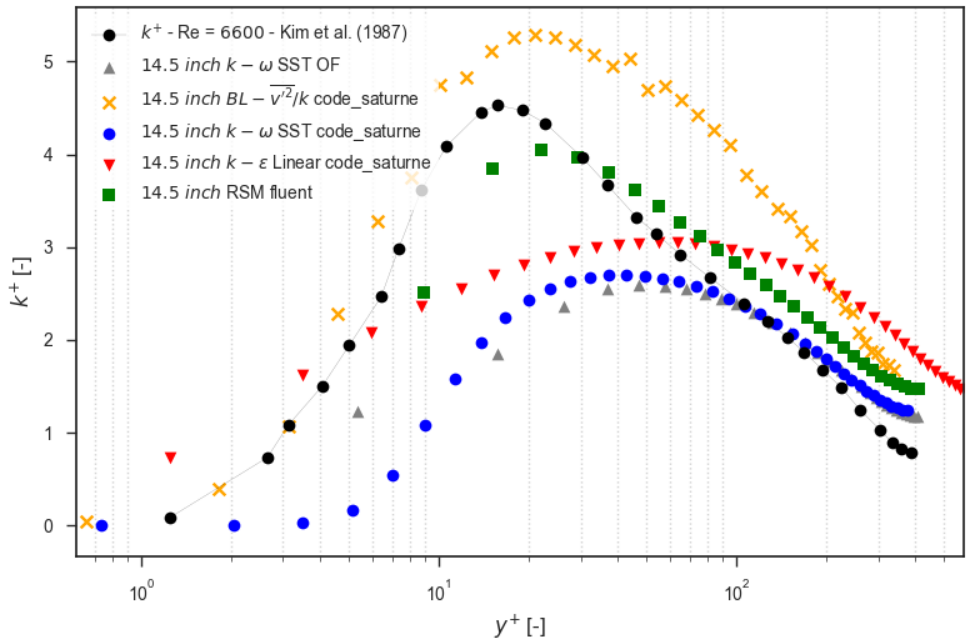

Figure 11: Non-dimensional turbulent kinetic energy in the 14.5 in. pipe

Figures 10 and 11 show the turbulent kinetic energy for this case in their dimensional and non-dimensional form, respectively. The $k-\varepsilon$ model in Code_Saturne largely over-predicts this quantity when compared to other models,

see Figure 10. When looking at the position of the peak of dimensionless turbulent intensity in Figure 11, the best matches with Kim *et al.* (1987) are obtained with the BL-v^2/k model of Code_Saturne and with the RSM of FLUENT. In terms of height, these two codes also agree better with the non-dimensional DNS estimates. For results obtained previously for a small diameter pipe, the BL-v^2/k also over-predicted the turbulent kinetic energy but showed a better estimate of the peak position and intensity than any other model tested, when compared to the DNS results from Kim *et al.* (1987).

Results obtained with the various turbulent models tested in the 14.5 in. pipe are summarized in Table 4. All codes estimates of friction velocity are close to the Blasius-based one, apart from those obtained with the $k-\varepsilon$ model in Code_Saturne. The same conclusions can be reached for the pressure gradient, with this code/model combination showing a poor agreement with the Blasius correlation.

Table 4: Simulation results for the 14.5 in. pipe

Turbulence model	Predicted friction velocity (m/s)		Predicted pressure gradient (Pa/m)
	manual	pressure-based	
BL-v^2/k (Code_Saturne)	0.0464	0.0519	25.43
$k-\omega$ SST (Code_Saturne)	0.0492	0.0480	21.73
$k-\omega$ SST (OpenFOAM)	0.0470	0.0520	25.49
$k-\varepsilon$ (Code_Saturne)	0.0895	0.0869	71.32
$RSM-LRR$ (FLUENT)	0.0482	0.0536	27.10
Blasius correlation	0.0508		24.37

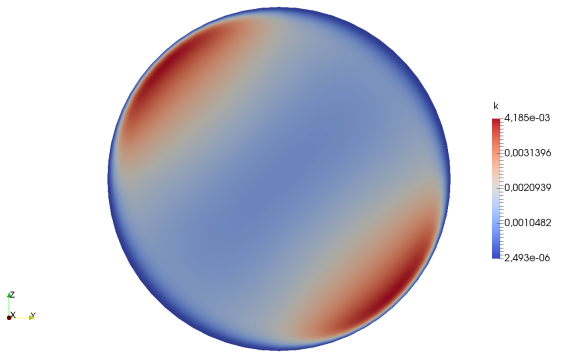

(a) Outlet distribution of k in the 14.5 in. pipe with Code_Saturne (BL-v^2/k model)

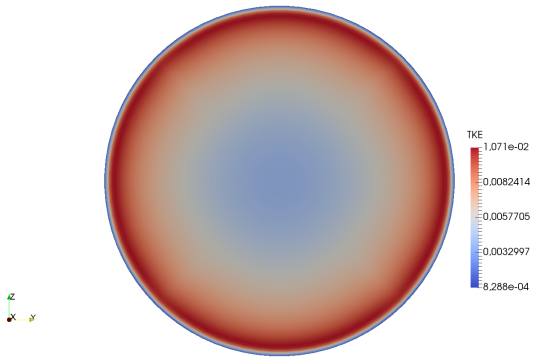

(b) Outlet distribution of k in the 14.5 in. pipe with FLUENT (RSM model)

Figure 12: Erroneous anisotropic prediction of the turbulent kinetic energy with Code_Saturne compared to the more realistic FLUENT distribution

It is worth noting that for an unknown reason, the turbulent kinetic energy pattern obtained with the BL-v^2/k model in Code_Saturne shows a strange anisotropy behaviour while the RSM in FLUENT shows a more realistic pattern, see Figure 12. Different meshes have been tested and periodic boundary conditions implemented. In all cases, a similar anisotropy was present when applying the BL-v^2/k model. As this phenomenon cannot be explained by the flow physics, it can only be assumed that this is due to a numerical problem in Code_Saturne. Further investigation would be required to understand and test this model further. However, this is out of the scope of the present work as

already available turbulence model have been used, without modification or alteration of the official implementation in the open source flow solvers.

6. 48 in. (≃ 1.219m) diameter pipe

Large diameter pipes are now investigated. Flow conditions used for the study of a vertical 48 in. diameter pipe are written in Table 5. When applying the Blasius correlation, a wall shear stress value around 1.7 Pa is obtained, which gives a friction velocity around 0.044 m/s.

Table 5: Flow conditions for oil in pipe

u (m/s)	ρ (kg/m^3)	μ $(Pa.s)$	Re $(-)$
0.84	873.47	2.0×10^{-2}	43,460

Once again, different meshes were used here. The first one comprises around 2.5M cells with $y^+ = 0.54$, and has been used for simulations performed in OpenFOAM with the $k-\omega$ SST turbulence model. The second one has nearly 1M cells, a y^+ value of 1.22. This mesh has been used for Code_Saturne with the $k-\omega$ SST model. The third mesh has also been generated for Code_Saturne, has been used with the BL-v^2/k model, comprises around 1.7M cells and displays a y^+ value of 0.89. For pipes of this size, the flow development length is longer than in previous cases. The pipe is therefore much longer here (100 m) than for the 0.5 in. diameter pipe (5 m) and the 14.5 in. diameter pipe (20 m).

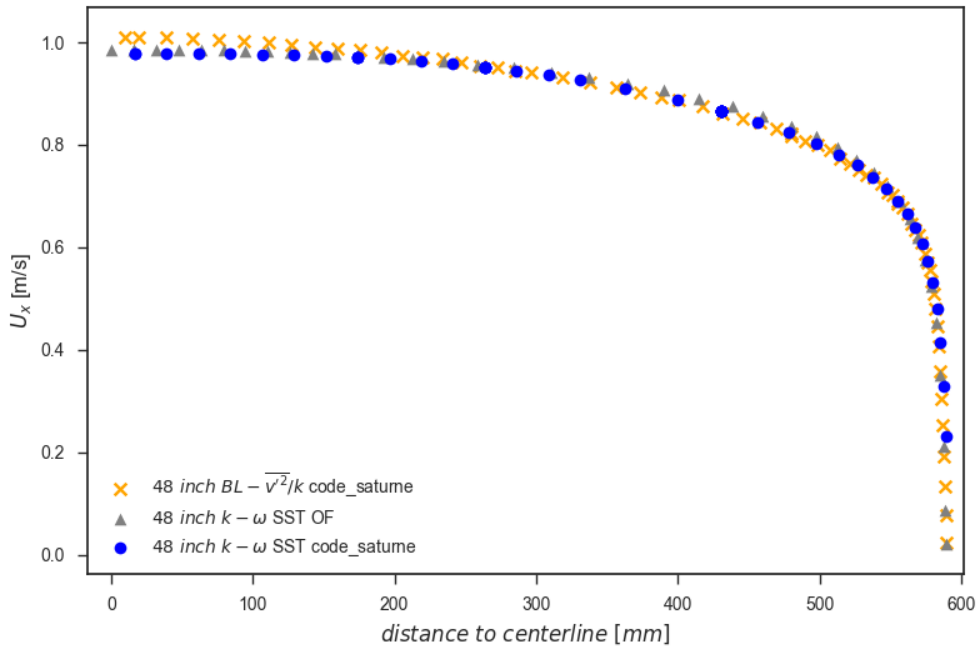

Figure 13: Axial velocity profiles in the 48 in. diameter pipe; comparison between $k-\omega$ SST and BL-v^2/k

Results obtained with the 48 in. pipe were qualitatively better than for the other ones detailed previously. One of the reasons is the high Reynolds number flow present in this pipe, where turbulence models are expected to be more

reliable. The turbulence model showing the best performances in small and medium pipes has been tested for the large pipe: the $k-\omega$ SST. The BL-v^2/k has also been investigated as the non-dimensional turbulent kinetic energy obtained with this model showed a fair agreement with DNS values from Kim *et al.* (1987) in 3 in. and 14.5 in. diameter pipes.

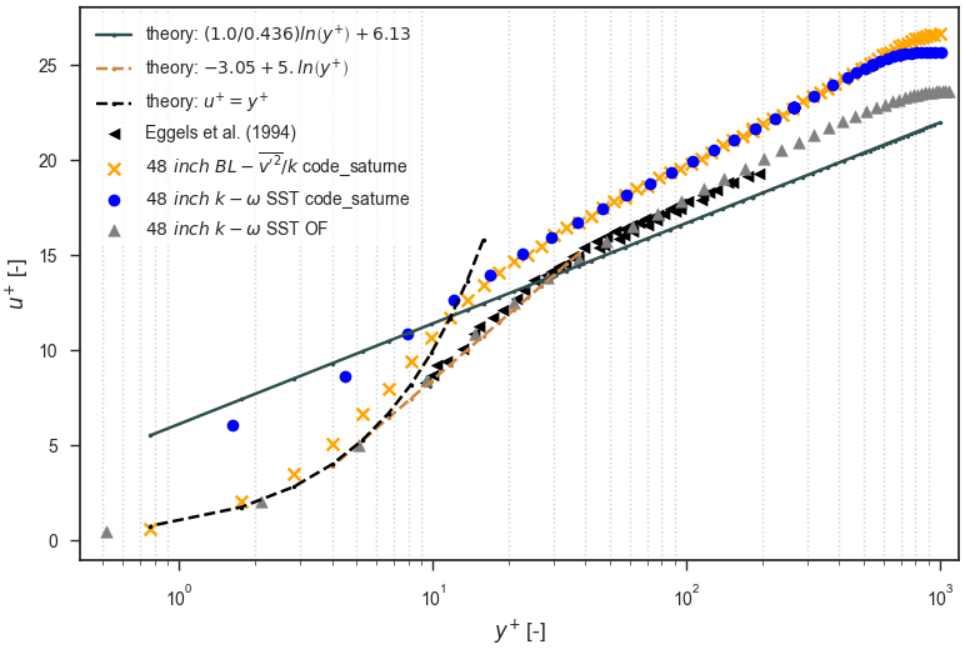

Figure 14: Non-dimensional axial velocity profiles in the 48 in. diameter pipe; comparison BL-v^2/k from Code_Saturne vs Eggels et al. (1994)

As can be seen in Figure 13, velocity profiles obtained from simulations performed with both turbulence models are similar. However, the BL-v^2/k model predicts a slightly larger mean velocity near the centreline of the pipe.

Non-dimensional velocities are compared to the theoretical values and to the experimental data reported in Eggels *et al.* (1994) in Figure 14. The OpenFOAM prediction is fairly close to the results from Eggels *et al.* (1994) and to the theoretical asymptotes. The overall non-dimensional velocity predicted by Code_Saturne is higher than the theoretical values, but evolves past $y^+ = 10$ with a slope comparable to the theoretical one. The two predictions from Code_Saturne are also nearly identical past $y^+ = 10$. It is likely that the near-wall spacing of the mesh used for the $k-\omega$ SST turbulence model in Code_Saturne is not refined enough to follow the usual $u^+ = y^+$ below $y^+ = 5$. It is assumed that if the mesh had been refined further near the wall (current $y^+ = 1.22$), the predicted u^* would have been resolved better and the non-dimensional plots would have shown a better agreement with the theoretical results. This statement is supported by the profile obtained with the same model in OpenFOAM, but this time with a $y^+ = 0.4$ which shows a closer match to the theoretical asymptotic curves.

Figure 15 describes the simulated non-dimensioned turbulent kinetic energy plotted against the DNS results from Kim *et al.* (1987). The $k-\omega$ SST model fails to correctly predict the turbulent kinetic energy, as it under-predicts the amplitude and the peak position is well above the value $y^+ \approx 16$. However, as for smaller diameter pipes, the BL-v^2/k model from Code_Saturne seems to have a better agreement with Kim *et al.* (1987). This model should probably be privileged when the study of the turbulent fields is important, for instance, when analysing particle dispersion and deposition.

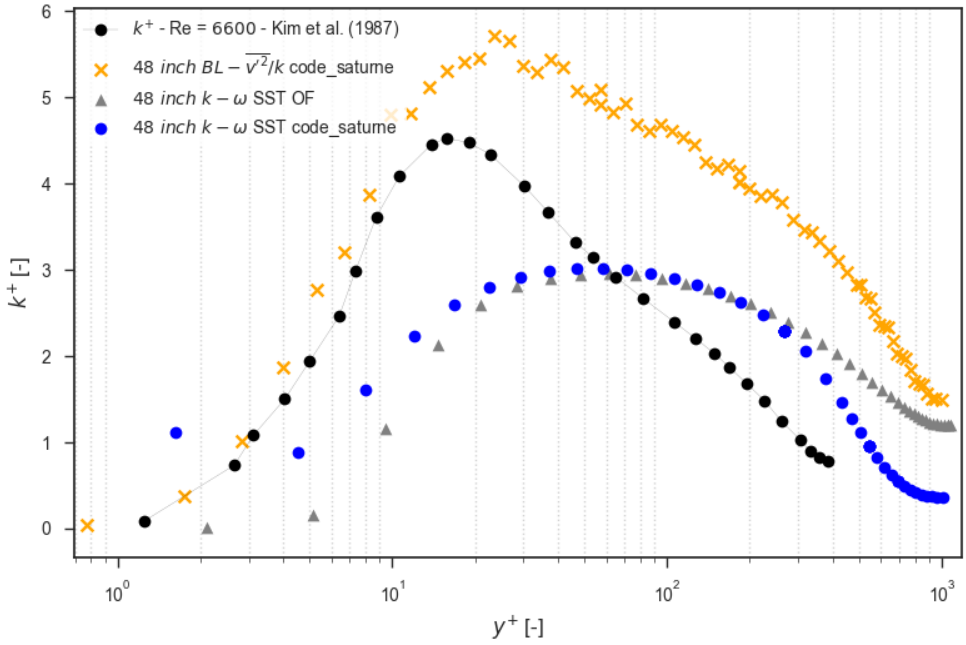

Figure 15: Non-dimensional turbulent kinetic energy in the 48 in. diameter pipe

The friction velocity and the pressure gradient from all simulations are reported in Table 6. All numerical results are in agreement with the Blasius correlation, the farthest estimates, although still acceptable, being this time obtained with the $k-\omega$ SST model in Code_Saturne.

Table 6: Simulation results for the 48 in. pipe

Turbulence model	Predicted friction velocity (m/s)		Predicted pressure gradient (Pa/m)
	manual	pressure-based	
BL-v^2/k (Code_Saturne)	0.0353	0.0458	6.19
$k-\omega$ SST (Code_Saturne)	0.0400	0.0390	4.50
$k-\omega$ SST (Open_FOAM)	0.0420	0.0414	5.07
Blasius correlation	0.0439		5.72

7. Conclusion

The RSM implemented in the commercial CFD code FLUENT seemed to out-pass all other turbulence models investigated in this work which are available in the open source CFD codes OpenFOAM and Code_Saturne. This model, used for simulations in 14.5 in. diameter pipes only, produced a good agreement with Blasius (friction velocity and pressure gradient), the theoretical asymptotic values of u^+, and experimental data from Eggels *et al.* (1994). In addition, the non-dimensional turbulent kinetic energy obtained with this model compared fairly well with DNS results from Kim *et al.* (1987). Such result was expected as the RSMl takes into account the full anisotropic turbulence of

the flow. The downside of using this model is the simulation time which is significantly longer than with any other turbulence model.

It has been established through this work that the commonly used turbulence models implemented in the open source CFD flow solvers OpenFOAM and Code_Saturne did not provide the same estimates of the non-dimensional turbulent kinetic energy as the DNS results from Kim *et al.* (1987). This could be inherent to the difficulties encountered for the evaluation of an accurate velocity gradient at the wall. If the mesh spacing next to the wal is not fine enough, the friction velocity is not well calculated, thus produces an erroneous non-dimensional representation of the turbulence kinetic energy, even if the dimensional representation is correct.

From all turbulence models tested with the open source codes which were less computationally expensive than the RSM in FLUENT, the $k-\omega$ SST was one of the most efficient in determining a friction velocity and a pressure gradient in agreement with the Blasius correlations. This model provided fairly good results in the small, medium and large diameter pipes. It can therefore be recommended for similar studies with both OpenFOAM and Code_Saturne. The BL-v^2/k turbulence model in Code_Saturne showed the best comparison with the DNS study of Kim *et al.* (1987) in all three pipes studied and provided the best match of friction velocity and pressure gradient with the Blasius correlations. However, discrepancies were observed for the non-dimensional velocity profiles when compared to the theoretical asymptotic curves and to Eggels *et al.* (1994), which are again attributed to the difficulties in obtaining an accurate friction velocity when using this model, and therefore alter the non-dimensional results.

This work is, to the authors' best knowledge, the first study aiming at evaluating the influence of commonly used turbulence models implemented in open source codes on the velocity and turbulent kinetic energy in large (14.5 in.) and very large (48 in.) pipes. No special effect due to the pipe diameter was seen on the velocity and turbulent kinetic energy when using the RANS solvers with a single phase flow. A scaling-up procedure from a laboratory-type pipe to an industrial-type pipe could therefore be established with RANS models. Note finally that none of the non-scaling features which can be defined in a DNS have been investigated in this work. The limit of applicability of this study is therefore for common RANS approaches.

Acknowledgments

The authors would like to thank the anonymous Reviewers and the Executive Editor of JPSE for their comments, suggestions and attention to details which highly improved the overall quality of this paper. This research did not receive any specific grant from funding agencies in the public, commercial, or not-for-profit sectors.

References

Ahn, Junsun, Lee, Jae Hwa, Lee, Jin, hoon Kang, Ji, & Sung, Hyung Jin. 2015. Direct numerical simulation of a 30R long turbulent pipe flow at $Re_\tau = 3008$. *Physics of Fluids*, **27**.

ANSYS, Inc. 2013. *Fluent 15.0 User's Guide*.

Benedict, Robert P. 1980. *Fundamentals of PIPE FLOW*. John Wiley & Sons, Inc.

Billard, F., & Laurence, D. 2012. A robust k--v2/k elliptic blending turbulence model applied to near-wall, separated and buoyant flows. *International Journal of Heat and Fluid Flow*, **33**(1), 45–58.

Billard, F., Laurence, D., & Osman, K. 2015. Adaptive Wall Functions for an Elliptic Blending Eddy Viscosity Model Applicable to Any Mesh Topology. *Flow, Turbulence and Combustion*, **94**(4), 817–842.

Brown, L., Hewitt, G.F., Hu, B., Thompson, C.P., & Verdin, P. 2009. Predictions of droplet distribution in low liquid loading, stratified flow in large diameter pipeline. *14th International Conference on Multiphase Production Technology, Cannes (France)*.

Code_Saturne. 2015. *Code_Saturne Theory Guide*.

Den Toonder, J. M. J., & Nieuwstadt, F. T. M. 1997. Reynolds number effects in a turbulent pipe flow for low to moderate Re. *Physics of Fluids*, **9**.

Eggels, J. G. M., Unger, F., Weiss, M. H., Westerweel, J., Adrian, R. J., Friedrich, R., & Nieuwstadt, F. T. M. 1994. Fully developed turbulent pipe flow: a comparison between direct numerical simulation and experiment. *Journal of Fluid Mechanics*, **268**, 175–210.

El Khoury, G. K., Schlatter, P., Brethouwer, G., & Johansson, A.V. 2014. Turbulent pipe flow: Statistics, Re-dependence, structures and similarities with channel and boundary layer flows. *Journal of Physics: Conference Series 506*.

Escue, A., & Cui, J. 2010. Comparison of turbulence models in simulating swirling pipe flows. *Applied Mathematical Modelling*, **34**(10), 2840–2849.

Gibson, M.M., & Launder, B.E. 1978. Ground Effects on Pressure Fluctuations in the Atmospheric Boundary Layer. *J. Fluid Mech.*, **86**, 491–511.

Guan, X., Zhao, Y., Wang, J., Jin, Y., & Zhang, D. 2015. Numerical analysis of quasi-steady flow characteristics in large diameter pipes with low liquid loading under high pressure. *Journal of Natural Gas Science and Engineering*, **26**, 907–920.

Hrenya, C.M., Bolio, E.J., Chakrabarti, D., & Sinclair, J.L. 1995. Comparison of low reynolds number k-epsilon turbulence models in predicting fully developed pipe flow. *Chemical Engineering Science*, **50**(12), 1923–1941.

Hultmark, M., Bailey, S. C. C., & Smits, A. J. 2010. Scaling of near-wall turbulence in pipe flow. *Journal of Fluid Mechanics*, **649**, 103–113.

Karvinen, A., & Ahlstedt, H. 2008. Comparison of turbulence models in case of three-dimensional diffuser. *Proceedings of Open Source CFD International Conference 2008*, 1–17.

Kim, J., Moin, P., & Moser, R. 1987. Turbulence statistics in fully developed channel flow at low Reynolds number. *Journal of Fluid Mechanics*, **177**, 133–166.

Launder, B.E., & Sharma, B.I. 1974. Application of the Energy-Dissipation Model of Turbulence to the Calculation of Flow Near a Spinning Disc. *Letters in Heat and Mass Transfer*, **1**(2), 131 – 138.

Launder, B.E., Reece, G.J., & Rodi, W. 1975. Progress in the development of a Reynolds-stress turbulence closure. *Journal of Fluid Mechanics*, **68**(3), 537–566.

Loyseau, X.F., & Verdin, P.G. 2016. Statistical model of transient particle dispersion and deposition in vertical pipes. *Journal of Aerosol Science*, **101**, 43–64.

Manceau, R., & Hanjalic, K. 2002. Elliptic blending model: A new near-wall Reynolds-stress turbulence closure. *Physics of Fluids*, **14**(2), 744–754.

Matida, E.A., Nishino, K., & Torii, K. 2000. Statistical simulation of particle deposition on the wall from turbulent dispersed pipe flow. *International Journal of Heat and Fluid Flow*, **21**(4), 389–402.

Menter, F.R. 1994. Two-equation eddy-viscosity turbulence models for engineering applications. *AIAA Journal*, **32**(8), 1598–1605.

Pope, S.B. 2001. *Turbulent Flows*.

Reynolds, O. 1883. An experimental investigation of the circumstances which determine whether the motion of water shall be direct or sinuous and the law of resistance in parallel channels. *Phil. Trans. R. Soc.*, **174**, 935–982.

Salehi, S., Raisee, M., & Cervantes, M. J. 2017. Computation of Developing Turbulent Flow through a Straight Asymmetric Diffuser with Moderate Adverse Pressure Gradient . *Journal of Applied Fluid Mechanics*, **10**(4), 1029–1043.

Salome. 2015. *User's Guide*.

Shawkat, M. E., Ching, C. Y., & Shoukri, M. 2008. Bubble and liquid turbulence characteristics of bubbly flow in a large diameter vertical pipe. *International Journal of Multiphase Flow*, **34**(8), 767–785.

Spalart, P. R. 2000. Strategies for turbulence modelling and simulations. *International Journal of Heat and Fluid Flow*, **21**(3), 252–263.

Verdin, P.G., Thompson, C.P., & Brown, L.D. 2014. CFD modelling of stratified/atomization gasliquid flow in large diameter pipes. *International Journal of Multiphase Flow*, **67**, 135–143.

Vijiapurapu, S., & Cui, J. 2010. Performance of turbulence models for flows through rough pipes. *Applied Mathematical Modelling*, **34**(6), 1458–1466.

Weller, H.G, & Tabor, G. 1998. A tensorial approach to computational continuum mechanics using object-oriented techniques. *Computers in Physics*, **12**(6), 620–631.

Wilcox, D.C. 1988. Re-assessment of the scale-determining equation for advanced turbulence models. *AIAA Journal*, **26**(11), 1299–1310.

Zagarola, M.V., Perry, A.E., & Smits, A.J. 1997. Log laws of power laws: The scaling in the overlap region. *Physics of Fluids*.